Terahertz V2I-aided Tracking Design

Zheng Lin*, Lifeng Wang*, Jie Ding*, Yuedong Xu*, and Bo Tan†
* Department of Electronic Engineering, Fudan University, Shanghai, China
†Faculty of Information Technology and Communication Sciences, Tampere University, Finland

***Abstract*—In this paper, we design the vehicle tracking in the terahertz (THz) vehicle-to-infrastructure (V2I) networks, where roadside units (RSUs) equipped with leaky-wave antennas help to estimate the driving states of multiple vehicles after receiving the vehicles' feedback. Different from the conventional phased arrays, the leaky-wave antenna has the potential of improving the sensing accuracy with lower system overhead thanks to its unique spatial-spectral coupling feature. The generalized mobile scenario is studied in which vehicles drive at time-varying speeds. A novel unscented Kalman filter (UKF) based solution is proposed to track the vehicles without requirement of addressing the Doppler effect. Simulation results confirm that the proposed tracking solution can evaluate the propagation angle, vehicle's states and inter-vehicle distance accurately.**

I. Introduction

Vehicle-to-infrastructure communications (V2I) play an essential role in supporting vehicle-to-everything (V2X) services [1] and intelligent transportation systems (ITS) [2]. The V2I-aided sensing and communication can assist robust automated driving with extended sensors [3]. With the development of 5G millimeter wave (mmWave) technology, vehicle positioning via mmWave V2I has been studied in vehicular networks [4–6]. Since THz transmission is one of 6G potential technologies [7], terahertz (THz) V2I with much wider channel bandwidths enable higher sensing accuracy and lower-latency communication than mmWave V2I [7, 8].

In THz systems, selecting appropriate type of antenna is crucial. Although phased arrays have been used in 5G mmWave systems, the implementation of them in the THz links are confronted with many challenging issues involving antenna scale [7], path discovery [9], feed network design [10] and beam squinting etc. Moreover, extensive beam training is required for phased arrays in the 5G mmWave setup, which may result in much higher latency in the THz systems [11]. Compared to the conventional phased arrays, easy-to-manufacture leaky-wave antennas are envisioned as a promising approach to establish cost-effective THz links [10, 12, 13]. The applications of leaky-wave antennas have been considered in many areas such as THz radar sensing [14] and THz frequency-division multiplexing communication [15] etc. One big characteristic of the leaky-wave antenna is that frequencies are coupled with the propagation angles, which can be exploited for designing more efficient path discovery and mobile object tracking [9, 16]. Based on this characteristic, a roadside unit (RSU) equipped with one single leaky-wave antenna can simultaneously estimate the inter-vehicle distance in multi-vehicle systems which have the capabilities of the adaptive cruise control (ACC) and cooperative ACC (CACC) [17]. In addition, differing from the beam management in the phased array systems [18], exhaustive beam scanning is unnecessary in the leaky-wave antenna systems as demonstrated in [9, 16]. Therefore, the use of leaky-wave antennas brings the great potential for improving sensing and communication efficiency in the THz V2I networks.

Channel tracking designs in the mmWave and THz cellular systems have been investigated in the literature [19–22]. It is shown in [19] that the extended Kalman filter (EKF) can be a low-complexity tracking filter in mmWave mobile environments. Meanwhile, an EKF-based tracking strategy is proposed to minimize the beam alignment error of the mmWave systems in [20]. The work of [21] focuses on the direction of arrival tracking with unscented Kalman filter (UKF) in the mmWave massive multiple-input multiple-output (MIMO) cellular systems, where a kinematic model of the direction of arrival is considered and the rotated spatial support indexes are the observations. To make fast THz channel tracking in the linear user motion model, [22] attempts to estimate the propagation angle with the assistance of the prior beamspace channel information in the THz massive MIMO cellular systems with conventional antenna arrays. The application of dual-functional radar-communication (DFRC) technique in the mmWave V2I networks is considered in [6], where an EKF based beam tracking scheme is proposed by addressing the case of vehicle driving at constant speed. Owing to the fact that THz sensing in the V2I networks is still in its infancy, this paper considers a generalized V2I scenario where vehicles drive at time-varying speeds, which has not been conducted yet. We develop a novel vehicle tracking method based on the THz V2I link with leaky-wave antenna. In such a significantly non-linear dynamic scenario, the EKF that adopts the first-order Taylor expansion for linearization can lead to large estimation errors. The UKF amends the flaw of EKF by using a deterministic sampling approach while keeping the same computational complexity as the EKF [23].

In the considered THz V2I network, we design an UKF-based approach such that a RSU equipped with a single leaky-wave antenna can track multiple vehicles and their inter-vehicle distances. Different from the kinematic models seen in the existing works, we consider the generalized V2I networks in which vehicles can drive at non-linear time-varying speeds. The designed vehicle tracking method is robust and insensitive to the Doppler shift compared to the tracking method with conventional phased arrays, since phase information is not required.

Notations: In this paper, $\mathrm{sinc}\,(x) = \sin(x)/x$ and

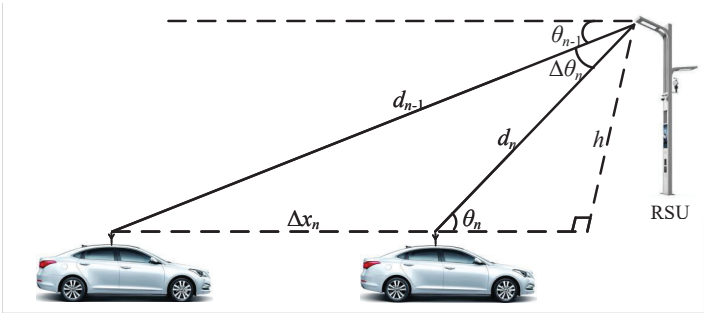

Fig. 1. An illustration of vehicle tracking.

$\operatorname{arccot}(x)$ is the inverse of cotangent function; $\mathbb{E}\{\cdot\}$ is the expectation operator; $(\cdot)^T$ is the transpose operator; $\operatorname{diag}(V)$ denotes the diagonal matrix whose diagonal elements are the entries of a vector V; $\mathbf{A}^{-1}$ is the inverse of the matrix $\mathbf{A}$.

II. System Descriptions

In the THz V2I network, the RSU equipped with a lowest transverse-electric (TE_1) mode leaky-wave antenna tracks multiple vehicles located in an arbitrary lane and each vehicle has one omnidirectional antenna. Based on [24], the far-field radiation pattern of TE_1 mode leaky-wave antenna can be calculated as

$$G(f,\theta) = \ell \operatorname{sinc}\left[\left(-j\alpha - k_0(f)\cos\theta + \beta(f)\right)\frac{\ell}{2}\right], \quad (1)$$

where f is the THz frequency, θ is the propagation angle ($0 < \theta < 90^o$), ℓ is the aperture length, $j = \sqrt{-1}$, α is the attenuation coefficient due to the power absorption in the structure, $k_0(f) = 2\pi f/c$ with the speed of light c is the wavenumber of the free-space, $\beta(f) = k_0(f)\sqrt{1-\left(\frac{f_{\mathrm{co}}}{f}\right)^2}$ is the phase constant of the TE_1 mode based traveling wave, in which $f_{\mathrm{co}} = \frac{c}{2L}$ with the inter-plate distance L is the cutoff frequency. Given a line-of-sight (LoS) direction θ of a vehicle, the maximum level of the radiation can be obtained by using the frequency as follows [25]:

$$f^{\max}(\theta) = \frac{f_{\mathrm{co}}}{\sin\theta}, \quad (2)$$

in other words, the frequency $f^{\max}(\theta)$ needs to be chosen in order to achieve the maximum level of the radiation at the direction θ. As shown in the following section, such a spatial-spectral coupling feature for leaky-wave antenna can be leveraged to improve the efficiency of vehicle tracking, due to the fact that the vehicles are spatially separated in practice.

Since each vehicle's states are estimated in the same fashion, we focus on an arbitrary vehicle for simplicity. As illustrated in Fig. 1, the geometric properties of a vehicle at the time $n-1$ and n are characterized as

$$\frac{h}{\sin\theta_{n-1}\sin\theta_n} = \frac{d_n}{\sin\theta_{n-1}} = \frac{d_{n-1}}{\sin\theta_n} = \frac{\Delta x_n}{\sin\Delta\theta_n}, \quad (3)$$

where h is the minimum communication distance and depends on the absolute antenna elevation difference and perpendicular distance between a vehicle in a lane and the RSU, θ_{n-1} and θ_n are the propagation angles, d_n and d_{n-1} are the communication distances at time n and $n-1$, respectively, $\Delta\theta_n = \theta_n - \theta_{n-1}$, and Δx_n is the moving distance from the time $n-1$ to n, which is calculated as

$$\Delta x_n = v_{n-1}\Delta\mathrm{T} + \frac{1}{2}a_{n-1}(\Delta\mathrm{T})^2. \quad (4)$$

In (4), v_{n-1} is the vehicle's velocity at the time $n-1$, $\Delta\mathrm{T}$ is the duration from the time $n-1$ to n, a_{n-1} is the acceleration/decerelation value at the time $n-1$, which is assumed to be at least constant in a time interval ($\Delta\mathrm{T}$). We first derive the dynamics of the angle of departure, based on (3), we have

$$\frac{d_{n-1}}{\sin\Delta\theta_n\cos\theta_{n-1} + \cos\Delta\theta_n\sin\theta_{n-1}} = \frac{\Delta x_n}{\sin\Delta\theta_n}. \quad (5)$$

After some manipulations, (5) is re-written as

$$\Delta\theta_n = \operatorname{arccot}\left(\frac{d_{n-1}}{\Delta x_n\sin\theta_{n-1}} - \cot\theta_{n-1}\right), \quad (6)$$

Since $d_n = \frac{\Delta x_n\sin\theta_{n-1}}{\sin\Delta\theta_n}$ and $\sin\Delta\theta \approx \Delta\theta_n$ with small $\Delta\theta_n$, d_n can be approximated as

$$d_n \approx \frac{\Delta x_n\sin\theta_{n-1}}{\Delta\theta_n} = \frac{\Delta x_n\sin\theta_{n-1}}{\operatorname{arccot}\left(\frac{d_{n-1}}{\Delta x_n\sin\theta_{n-1}} - \cot\theta_{n-1}\right)}. \quad (7)$$

In light of (4), (6) and (7), the dynamical model for state evolution over the time is written as follows:

$$\begin{cases} v_n = \ v_{n-1} + a_{n-1}\Delta\mathrm{T} + u_v, \\ \theta_n = \theta_{n-1} + \operatorname{arccot}\left(\frac{(\sin\theta_{n-1})^{-1}d_{n-1}}{v_{n-1}\Delta\mathrm{T}+\frac{1}{2}a_{n-1}(\Delta\mathrm{T})^2} - \cot\theta_{n-1}\right) + u_\theta, \\ d_n = \frac{\left(v_{n-1}\Delta\mathrm{T}+\frac{1}{2}a_{n-1}(\Delta\mathrm{T})^2\right)\sin\theta_{n-1}}{\operatorname{arccot}\left(d_{n-1}\left(\left(v_{n-1}\Delta\mathrm{T}+\frac{1}{2}a_{n-1}(\Delta\mathrm{T})^2\right)\sin\theta_{n-1}\right)^{-1} - \cot\theta_{n-1}\right)} + u_d, \end{cases} \quad (8)$$

where u_v, u_θ and u_d are the process noises with zero mean and their variances are σ_v^2, σ_θ^2 and σ_d^2, respectively[1]. The considered kinematic model given by (8) is generalized where vehicles drive at non-linear time-varying speeds.

It has been confirmed in [26] that the THz network with leaky-wave antennas is noise-limited and co-channel interference is negligible. Therefore, the sounding signal received at a vehicle is given by

$$y(t) = \sqrt{p\widetilde{G}(f(t),\theta(t))}\hbar z(t-\tau_n)\, e^{j2\pi f_{\mathrm{Doppler}}(t)t} + \varpi_y(t). \quad (9)$$

In (9), p is the transmit power, $\widetilde{G}(f(t),\theta(t)) = \xi G(f(t),\theta(t))$ is the effective antenna gain in which ξ can be easily obtained by measuring the effective antenna gain for a particular leaky-wave antenna structure and known a priori, $\hbar$ is the THz channel coefficient, $z(t)$ with $\mathbb{E}\{z(t)z^H(t)\} = 1$ is the sounding signal, τ_n is the propagation delay, $f_{\mathrm{Doppler}}(t)$ is the Doppler shift at time t, $\varpi_y(t)$ is the complex additive

[1]Note that these process noises have been assumed to follow Gaussian distributions in some works such as [19].

white Gaussian noise with zero mean and variance σ_y^2, which is independent of the process noises in (8).

Remark 1: Different from the sensing systems with large phased arrays where multiple orthogonal narrow beams are generated to track several vehicles, the leaky-wave antenna's spatial-spectral coupling effects (signatures) enable that multiple vehicles can be identified by exploiting their unique link directions without a need for beam association. In practice, the sounding signal can be formed as a moderate "THz rainbow" [9], which only needs to consist of signal components in directions of interest (not all directions), thanks to the known prior link direction information during the tracking process.

III. Vehicle Tracking Design

In this section, we propose a new design on vehicle tracking via THz links. In contrast to the traditional phased array systems where the Doppler effect needs to be stringently evaluated in order to offer a better estimate of the propagation angle (namely sensitive to the Doppler effect), the spatial-spectral coupling feature of the leaky-wave antenna provides us a better tracking design without requiring the Doppler shift information. Specifically, based on (9), we observe the received signal strength (RSS) as

$$\overline{y}_n = p\widetilde{G}\left(f_n, \theta_n\right)|\hbar|^2 + \overline{\omega}_y, \tag{10}$$

where $\overline{\omega}_y \sim \exp\left(\lambda\right)$ is the exponential random variable with the parameter $\lambda = 1/\sigma_y^2$. Without loss of generality, we replace $\overline{\omega}_y$ with $\widetilde{\omega}_y = \overline{\omega}_y - \sigma_y^2$ for facilitating the derivations such that zero mean is kept. In addition, it is noted that the channel power gain $|\hbar|^2$ can be easily extracted from the RSS in the coherence time. To improve the accuracy of the distance measurement, the propagation delay is also observed as

$$\tau_n = \frac{d_n}{c} + \varpi_\tau, \tag{11}$$

where c is the speed of light, ϖ_τ is the noise perturbation with zero mean and its variance σ_τ^2. Thus the observation model can be written as

$$\mathbf{\Xi}_n = \varphi\left(\mathbf{S}_n\right) + \boldsymbol{\varpi}_n, \tag{12}$$

where $\mathbf{\Xi}_n = \left[\overline{y}_n, \tau_n\right]^T$ is the observation vector, $\varphi\left(\cdot\right)$ is the mapping function defined by (10) and (11), $\mathbf{S}_n = \left[v_n, \theta_n, d_n\right]^T$ is the state vector and $\boldsymbol{\varpi}_n = \left[\overline{\omega}_y, \varpi_\tau\right]^T$ are the noise vector. Likewise, the state evolution model is

$$\mathbf{S}_n = \psi\left(\mathbf{S}_{n-1}\right) + \mathbf{u}_n, \tag{13}$$

where $\psi\left(\cdot\right)$ is defined by (8) and $\mathbf{u}_n = \left[u_v, u_\theta, u_d\right]^T$.

As indicated from (12) and (13), both the state evolution model and the observation model are real-valued and highly non-linear. Although the EKF and UKF have the same order of computational complexity [23], the UKF can overcome the approximation issues of the EKF in the non-linear systems. Therefore, we propose a UKF-based approach to estimate the states in a recursive manner, which is concluded as follows:

1) Initialization: The initial estimate of the propagation angle $\hat{\theta}_\circ$ can be obtained by using the detection scheme with a leaky-wave antenna in [16] where training is not required. Since the use of very large THz bandwidths enables highly accurate observation of the propagation delay[2], the communication distance is initialized as $\hat{d}_\circ = c\tau_\circ$ according to (11). The initial speed value $\hat{v}_\circ$ can be measured by the vehicle's odometer and the acceleration/deceleration value can be set as an arbitrary constant. Therefore, the initial state vector is $\hat{\mathbf{S}}_\circ = \mathbb{E}\{\mathbf{S}_\circ\} = \left[\hat{v}_\circ, \hat{\theta}_\circ, \hat{d}_\circ\right]^T$ and its covariance $\mathbf{C}_{\hat{\mathbf{S}}_\circ} = \mathbf{\Lambda_u} = \mathrm{diag}\left(\left[\sigma_v^2, \sigma_\theta^2, \sigma_d^2\right]^T\right)$ ($\mathbf{\Lambda_u}$ is the covariance of the process noise vector).

2) Statistics evaluation based on unscented transformation (UT): Unlike the EKF that needs linearized transformation via Taylor series, the UKF utilizes the UT method to directly estimate the statistics of a random variable in the non-linear systems. Specifically, let N denote the dimension of the state vector $\mathbf{S}_n$ (namely $N = 3$ in this paper), $2N+1$ symmetric sigma vectors around $\hat{\mathbf{S}}_{n-1}$ are chosen as follows:

$$\boldsymbol{\chi}_i = \begin{cases} \hat{\mathbf{S}}_{n-1},\ i = 0, \\ \hat{\mathbf{S}}_{n-1} + \sqrt{N+\varrho}\mathbf{L}_{n-1}\left(:, i\right),\ i = 1, \cdots, N, \\ \hat{\mathbf{S}}_{n-1} - \sqrt{N+\varrho}\mathbf{L}_{n-1}\left(:, i-N\right),\ i = N+1, \cdots, 2N, \end{cases} \tag{14}$$

where $\varrho = \epsilon^2\left(N + \varsigma\right) - N$, here ϵ is a small positive value [23] and ς is usually set to $3 - N$ [27], $\mathbf{L}_{n-1}\left(:, m\right)$ is the m-th column of $\mathbf{L}_{n-1}$ with $\mathbf{L}_{n-1}\mathbf{L}_{n-1}^T = \mathbf{C}_{\hat{\mathbf{S}}_{n-1}}$. According to UT, the state vector is predicted to be a weighted combination of these sigma vectors, which is given by

$$\hat{\mathbf{S}}_{n|n-1} = \frac{\varrho}{N+\varrho}\boldsymbol{\chi}_{0,n|n-1} + \sum_{i=1}^{2N}\frac{\boldsymbol{\chi}_{i,n|n-1}}{2\left(N+\varrho\right)}, \tag{15}$$

where $\boldsymbol{\chi}_{0,n|n-1} = \psi\left(\boldsymbol{\chi}_0\right)$, $\boldsymbol{\chi}_{i,n|n-1} = \psi\left(\boldsymbol{\chi}_i\right)$. The covariance of $\hat{\mathbf{S}}_{n|n-1}$ is calculated as

$$\begin{aligned}\mathbf{C}_{\hat{\mathbf{S}}_{n|n-1}} = {} & w_0\left(\boldsymbol{\chi}_{0,n|n-1} - \hat{\mathbf{S}}_{n|n-1}\right)\left(\boldsymbol{\chi}_{0,n|n-1} - \hat{\mathbf{S}}_{n|n-1}\right)^T \\ & + \sum_{i=1}^{2N}\frac{\left(\boldsymbol{\chi}_{i,n|n-1} - \hat{\mathbf{S}}_{n|n-1}\right)\left(\boldsymbol{\chi}_{i,n|n-1} - \hat{\mathbf{S}}_{n|n-1}\right)^T}{2\left(N+\varrho\right)} + \mathbf{\Lambda_u},\end{aligned} \tag{16}$$

where $w_o = \frac{\varrho}{N+\varrho} + \left(1 - \epsilon^2 + \vartheta\right)$ with the commonly-seen $\vartheta = 2$. Similarly, the corresponding predicted observation vector is given by

$$\hat{\mathbf{\Xi}}_{n|n-1} = \frac{\varrho}{N+\varrho}\varphi\left(\boldsymbol{\chi}_{0,n|n-1}\right) + \sum_{i=1}^{2N}\frac{\varphi\left(\boldsymbol{\chi}_{i,n|n-1}\right)}{2\left(N+\varrho\right)}, \tag{17}$$

and its covariance is calculated as (18) (at the top of next page), in which $\mathbf{\Lambda}_{\boldsymbol{\varpi}} = \mathrm{diag}\left(\left[\sigma_y^4, \sigma_\tau^2\right]^T\right)$. The cross-covariance of $\hat{\mathbf{S}}_{n|n-1}$ and $\hat{\mathbf{\Xi}}_{n|n-1}$ is given by (19).

3) Kalman filter gain:

$$\mathcal{K}_n = \mathbf{C}_{\hat{\mathbf{S}}_{n|n-1}, \hat{\mathbf{\Xi}}_{n|n-1}}\mathbf{C}_{\hat{\mathbf{\Xi}}_{n|n-1}}^{-1}. \tag{20}$$

[2]The evaluation of propagation delay can be achieved in the initial access or synchronization phase via synchronization or reference signals.

$$\mathbf{C}_{\hat{\boldsymbol{\Xi}}_{n|n-1}} = w_0 \left(\varphi\left(\boldsymbol{\chi}_{0,n|n-1}\right) - \hat{\boldsymbol{\Xi}}_{n|n-1}\right)\left(\varphi\left(\boldsymbol{\chi}_{0,n|n-1}\right) - \hat{\boldsymbol{\Xi}}_{n|n-1}\right)^T + \sum_{i=1}^{2N} \frac{\left(\varphi\left(\boldsymbol{\chi}_{i,n|n-1}\right) - \hat{\boldsymbol{\Xi}}_{n|n-1}\right)\left(\varphi\left(\boldsymbol{\chi}_{i,n|n-1}\right) - \hat{\boldsymbol{\Xi}}_{n|n-1}\right)^T}{2\left(N+\varrho\right)} + \boldsymbol{\Lambda}_{\boldsymbol{\varpi}}, \tag{18}$$

$$\mathbf{C}_{\hat{\mathbf{S}}_{n|n-1},\hat{\boldsymbol{\Xi}}_{n|n-1}} = w_0 \left(\boldsymbol{\chi}_{0,n|n-1} - \hat{\mathbf{S}}_{n|n-1}\right)\left(\varphi\left(\boldsymbol{\chi}_{0,n|n-1}\right) - \hat{\boldsymbol{\Xi}}_{n|n-1}\right)^T + \sum_{i=1}^{2N} \frac{\left(\boldsymbol{\chi}_{i,n|n-1} - \hat{\mathbf{S}}_{n|n-1}\right)\left(\varphi\left(\boldsymbol{\chi}_{i,n|n-1}\right) - \hat{\boldsymbol{\Xi}}_{n|n-1}\right)^T}{2\left(N+\varrho\right)}, \tag{19}$$

4) State estimation:

$$\hat{\mathbf{S}}_n = \hat{\mathbf{S}}_{n|n-1} + \mathcal{K}_n\left(\boldsymbol{\Xi}_n - \hat{\boldsymbol{\Xi}}_{n|n-1}\right). \tag{21}$$

5) State covariance:

$$\mathbf{C}_{\hat{\mathbf{S}}_n} = \mathbf{C}_{\hat{\mathbf{S}}_{n|n-1}} - \mathcal{K}_n \mathbf{C}_{\hat{\boldsymbol{\Xi}}_{n|n-1}} \mathcal{K}_n^T. \tag{22}$$

Remark 2: It is obviously seen that the proposed vehicle tracking design with leaky-wave antenna is derivative-free. The size of the real covariance matrix for the predicted observed variables (only 2×2 in this design) is less than the traditional methods with large phased arrays in which Doppler shift is an important factor and may need to be precisely measured in practice. Therefore, the inverse of the real covariance matrix for Kalman filter gain calculation given by (20) can be computed with much lower level of complexity.

IV. Simulation Results

This section provides numerical results to confirm the efficiency of the proposed tracking design in Section III . In the simulations, the leaky-wave antenna's parameters include the aperture length $\ell = 0.045$m and the inter-plate distance $L = 3.5$mm. The observation time interval $\Delta \mathrm{T} = 20$ms, the transmit power is $p = 30$dBm, the minimum communication distance between a vehicle and the RSU is $h = 5$m. Without loss of generality, we provide an example of tracking one vehicle. The initial states of the considered vehicle include the velocity $v_\circ = 20$m/s, the direction $\theta_\circ = 5^\circ$ and thus the initial communication distance $d_\circ = h/\sin\theta_\circ = 57.36$m. The vehicle's acceleration remains constant within one observation time interval and changes following the Gaussian distribution with the mean a_{E} and the variance 9×10^{-4} (namely $a \sim \mathcal{N}\left(a_{\mathrm{E}}, 9 \times 10^{-4}\right)$) in the next observation time. The free-space path loss (FSPL) model is utilized since it can well predict the channel of LoS THz link for low range transmissions [7, 28]. The variances of the process noises in the state evolution model (8) are $\sigma_v^2 = 1 \times 10^{-2}$, $\sigma_\theta^2 = 4 \times 10^{-4}$ and $\sigma_d^2 = 2.5 \times 10^{-3}$, respectively, and the variances of the noises in the observation model are $\sigma_y^2 = 9 \times 10^{-2}$ and $\sigma_\tau^2 = 4 \times 10^{-20}$, respectively. The other simulation parameters are detailed in the following simulation results.

A. Comparisons with Cramer-Rao Lower Bound

In this subsection, we investigate the performance behaviors of the proposed tracking solution and Cramer-Rao lower bound (CRLB) in terms of the root mean square error (RMSE), to further demonstrate the efficiency of our tracking design. It is known that CRLB is the lower bound on the mean square error (MSE) of any unbiased estimator and can be easily obtained by following the approach mentioned in [29, Appendix 3B]. In the simulations, the root of the CRLB is the benchmark, the acceleration's mean is assumed to be $a_{\mathrm{E}} = 5\mathrm{m/s}^2$.

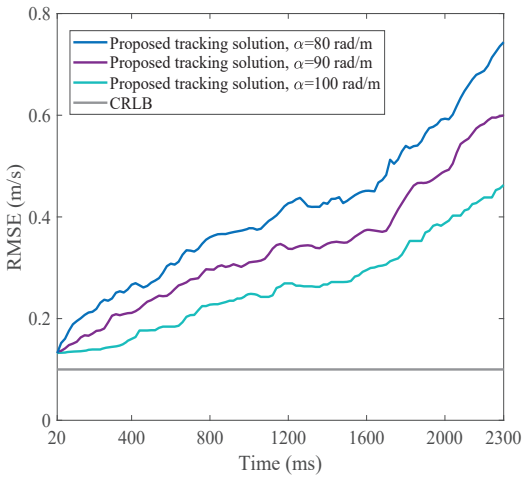

Fig. 2. The root mean square error (RMSE) for estimating the velocity.

Fig. 2 shows the RMSE of the estimated velocity achieved by the proposed tracking solution and the CRLB. We first see that slightly increasing the leaky-wave antenna's attenuation coefficient can reduce the estimation error. The reason is that the receive signal power is enhanced and thus the adverse effect of the noise in the RSS observation becomes less severe. Although the CRLB gives the lowest level of RMSE in this case, the proposed tracking solution still performs a much lower level of RMSE when noting that the vehicle's initial velocity is $v_\circ = 20$m/s. The performance gap between the proposed tracking solution and the CRLB increases over the time.

This is because that the proposed tracking design relies on the prior state information, but the vehicle's states change much faster between two consecutive observations when its velocity is higher, which makes the state and observation predictions less accurate based on the prior state information. To improve the estimation accuracy in the scenario with significantly high mobility, increasing tracking frequency (shorter observation time interval) may be required, however, the tradeoff between tracking frequency and system overhead needs to be balanced in practice.

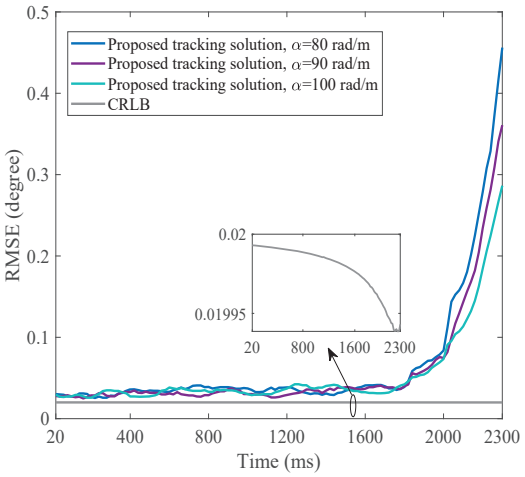

Fig. 3. The root mean square error (RMSE) for estimating the propagation angle.

Fig. 3 shows the RMSE of the estimated propagation angle achieved by the proposed tracking solution and the CRLB. By exploiting the leaky-wave antenna's spatial-spectral coupling effects, the performance of our tracking design is close to the CRLB when the vehicle's velocity is below a critical value. Another reason is that the Doppler effect caused by mobility is irrelevant to the estimation in our tracking solution since the Doppler shift observation is unnecessary. The estimation error decreases when slightly increasing the leaky-wave antenna's attenuation coefficient because of the stronger received signal power. As mentioned before, higher mobility leads to the rapid variations of the vehicle's states, which deteriorate the state and observation predictions.

Fig. 4 shows the RMSE of the estimated V2I communication distance achieved by the proposed tracking solution and the CRLB. The performance gap between the proposed tracking solution and the CRLB is marginal. Again, we see that slightly increasing the leaky-wave antenna's attenuation coefficient improves the estimation accuracy.

B. Inter-vehicle Distance Estimation

In this subsection, we consider that the RSU is connected to three vehicles located in the same lane as shown in Fig. 5, where vehicle 1's initial states include the velocity $v_{1,\circ} = 20$m/s, the direction $\theta_{1,\circ} = 6.2°$ and the mean of its acceleration $a_{1,\mathrm{E}} = 4.5\mathrm{m/s}^2$; vehicle 2's initial states include the

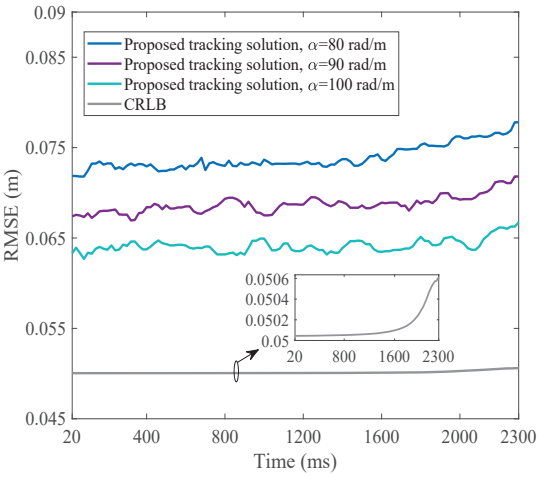

Fig. 4. The root mean square error (RMSE) for estimating the V2I communication distance.

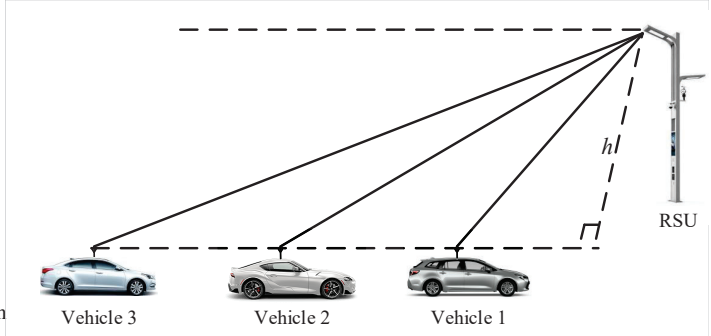

Fig. 5. An illustration of three vehicles connected to the RSU.

velocity $v_{2,\circ} = 20$m/s, the direction $\theta_{2,\circ} = 5.6°$ and the mean of its acceleration $a_{2,\mathrm{E}} = 4\mathrm{m/s}^2$; and vehicle 3's initial states include the velocity $v_{3,\circ} = 20$m/s, the direction $\theta_{3,\circ} = 5°$ and the mean of its acceleration $a_{3,\mathrm{E}} = 3.5\mathrm{m/s}^2$. The leaky-wave antenna's attenuation coefficient is $\alpha = 90$rad/m.

Fig. 6 shows the root mean square error (RMSE) for estimating the inter-vehicle distance. It is seen that by using our tracking design, the estimation error is minimal and increases slowly during the acceleration phase. Since vehicle 1 and vehicle 2 move faster than vehicle 3, the error of estimating the distance between vehicle 1 and vehicle 2 is larger than that between vehicle 2 and vehicle 3, and the error is further enlarged by estimating the longer distance between vehicle 1 and vehicle 3.

V. Conclusions

In the multi-vehicle THz V2I networks, vehicle tracking play a key role in the intelligent V2X communications. With the assistance of the angle-frequency coupling of leaky-wave antenna, we designed a UKF-based tracking solution to estimate the vehicle's velocity, direction and communication distance. Different from the existing methods, our design did not require the measurements of the Doppler shift. Simulation results have confirmed the efficiency of the proposed track-

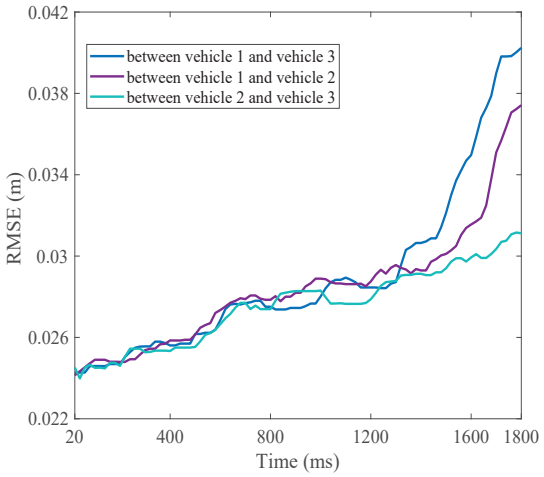

Fig. 6. The root mean square error (RMSE) for estimating the inter-vehicle distance with the transmit power $p = 30$dBm and $h = 5$m.

ing solution and shown that our performance with moderate tracking frequency is close to the CRLB when the vehicle's velocity is not significantly high.

REFERENCES

[1] 3GPP TS 22.185, "Service requirements for V2X services; Stage 1 (Release 16)," July 2020.

[2] Y.-Y. Lin and I. Rubin, "Infrastructure aided networking and traffic management for autonomous transportation," in *IEEE Inf. Theory Appl. Workshop (ITA)*, 2017, pp. 1–7.

[3] Y. Wang, G. de Veciana, T. Shimizu, and H. Lu, "Deployment and performance of infrastructure to assist vehicular collaborative sensing," in *IEEE VTC*, 2018, pp. 1–5.

[4] H. Wymeersch, G. Seco-Granados, G. Destino, D. Dardari, and F. Tufvesson, "5G mmwave positioning for vehicular networks," *IEEE Wireless Commun.*, vol. 24, no. 6, pp. 80–86, Dec. 2017.

[5] N. Gonzalez-Prelcic, R. Mendez-Rial, and R. W. Heath, "Radar aided beam alignment in mmwave V2I communications supporting antenna diversity," *Proc. Inf. Theory Appl. Workshop (ITA)*, Jan. 2016, pp. 1–7.

[6] F. Liu, W. Yuan, C. Masouros, and J. Yuan, "Radar-assisted predictive beamforming for vehicular links: Communication served by sensing," *IEEE Trans. Wireless Commun.*, vol. 19, no. 11, pp. 7704–7719, Nov. 2020.

[7] T. S. Rappaport *et al.*, "Wireless communications and applications above 100 GHz: Opportunities and challenges for 6G and beyond," *IEEE Access*, vol. 7, pp. 78 729–78 757, June 2019.

[8] H. Sarieddeen, N. Saeed, T. Y. Al-Naffouri, and M.-S. Alouini, "Next generation terahertz communications: A rendezvous of sensing, imaging, and localization," *IEEE Commun. Mag.*, vol. 58, no. 5, pp. 69–75, May 2020.

[9] Y. Ghasempour, C. Yeh, R. Shrestha, D. Mittleman, and E. Knightly, "Single shot single antenna path discovery in THz networks," in *Proc. 26th MobiCom*, 2020, pp. 1–13.

[10] D. Headland, Y. Monnai, D. Abbott, C. Fumeaux, and W. Withayachumnankul, "Tutorial: Terahertz beamforming, from concepts to realizations," *APL Photonics*, vol. 3, no. 5, pp. 1–32, 2018.

[11] M. Polese, J. M. Jornet, T. Melodia, and M. Zorzi, "Toward end-to-end, full-stack 6G terahertz networks," *IEEE Commun. Mag.*, vol. 58, no. 11, pp. 48–54, Nov. 2020.

[12] D. R. Jackson and A. A. Oliner, "Leaky-wave antennas," in Modern Antenna Handbook, C. Balanis, Ed. New York: Wiley, 2008.

[13] C.-Y. Yeh, Y. Ghasempour, Y. Amarasinghe, D. M. Mittleman, and E. W. Knightly, "Security in terahertz WLANs with leaky wave antennas," in *ACM WiSec*, 2020, pp. 1–11.

[14] H. Matsumoto, I. Watanabe, A. Kasamatsu, and Y. Monnai, "Integrated terahertz radar based on leaky-wave coherence tomography," *Nature Electronics*, vol. 3, pp. 122–129, Feb. 2020.

[15] N. J. Karl, R. W. McKinney, Y. Monnai, R. Mendis, and D. M. Mittleman, "Frequency-division multiplexing in the terahertz range using a leaky-wave antenna," *Nature Photonics*, vol. 9, pp. 717–721, Sept. 2015.

[16] Y. Ghasempour, C. Yeh, R. Shrestha, Y. Amarasinghe, D. Mittleman, and E. Knightly, "LeakyTrack: Non-coherent single-antenna nodal and environmental mobility tracking with a leaky-wave antenna," in *Proc. 18th ACM SenSys*, 2020, pp. 1–13.

[17] S. Darbha, S. Konduri, and P. R. Pagilla, "Benefits of V2V communication for autonomous and connected vehicles," *IEEE Trans. Intell. Transp. Syst.*, vol. 20, no. 5, pp. 1954–1963, May 2019.

[18] Y. Heng, J. G. Andrews, J. Mo, V. Va, A. Ali, B. L. Ng, and J. C. Zhang, "Six key challenges for beam management in 5.5G and 6G systems," *IEEE Commun. Mag.*, vol. 59, no. 7, pp. 74–79, July 2021.

[19] V. Va, H. Vikalo, and R. W. Heath, "Beam tracking for mobile millimeter wave communication systems," in *IEEE Global Conf. Signal and Inf. Process. (GlobalSIP)*, 2016, pp. 743–747.

[20] S. Jayaprakasam, X. Ma, J. W. Choi, and S. Kim, "Robust beam-tracking for mmwave mobile communications," *IEEE Commun. Letters*, vol. 21, no. 12, pp. 2654–2657, Dec. 2017.

[21] J. Zhao, F. Gao, W. Jia, S. Zhang, S. Jin and H. Lin, "Angle domain hybrid precoding and channel tracking for millimeter wave massive MIMO systems," *IEEE Trans. Wireless Commun.*, vol. 16, no. 10, pp. 6868–6880, Oct. 2017.

[22] X. Gao, L. Dai, Y. Zhang, T. Xie, X. Dai, and Z. Wang, "Fast channel tracking for terahertz beamspace massive MIMO systems," *IEEE Trans. Veh. Technol.*, vol. 66, no. 7, pp. 5689–5696, 2017.

[23] E. A. Wan and R. van der Merwe, *The Unscented Kalman Filter*, John Wiley & Sons, Inc., 2001.

[24] A. Sutinjo, M. Okoniewski, and R. H. Johnston, "Radiation from fast and slow traveling waves," *IEEE Antennas Propag. Mag.*, vol. 50, no. 4, pp. 175–181, Aug. 2008.

[25] D. R. Jackson, C. Caloz, and T. Itoh, "Leaky-wave antennas," *Proc. IEEE*, vol. 100, no. 7, pp. 2194–2206, July 2012.

[26] Z. Lin, L. Wang, B. Tan, and X. Li, "Spatial-spectral Terahertz Networks," *arXiv preprint arXiv:2101.02868v3*, Apr. 2021.

[27] S. Julier, J. Uhlmann, and H. F. Durrant-Whyte, "A new method for the nonlinear transformation of means and covariances in filters and estimators," *IEEE Trans. Automat. Contr.*, vol. 45, no. 3, pp. 477–482, Mar. 2000.

[28] J. Kokkoniemi, J. Lehtomäki, and M. Juntti, "A line-of-sight channel model for the 100-450 gigahertz frequency band," *EURASIP J. Wireless Com Network*, pp. 1–15, Apr. 2021.

[29] S. M. Kay, *Fundamentals of Statistical Signal Processing: Estimation Theory*, vol. 1. Englewood Cliffs, NJ, USA: Prentice-Hall, 1998.